Proposal of a Method for Estimating Needle Base Position to Decrease Needle Deflection During Robotic Needle Insertion Using Machine Learning

Axel Yap Shen Yit[1], Yuta Fukushima[1]

[1]Teikyo University, Graduate School of Science and Engineering, Utsunomiya, Tochigi, Japan

24FM10022wb@stu.teikyo-u.ac.jp, fukushima@ics.teikyo-u.ac.jp

1. Introduction

1.1 Background

Needle insertion, a fundamental medical technique for puncturing the human body, is an essential skill that must be mastered. Needle insertion is performed on various sites and tissues, including blood vessels such as veins and arteries, organs such as the liver, intestines, breasts, brain, and prostate, and cavities such as the epidural and pericardial spaces. Additionally, its applications are diverse, ranging from biopsy and treatment to drainage of accumulated fluids, making it a crucial procedure in many medical interventions. One of the most common needle insertion procedures is venipuncture for blood sampling from the arm's veins, which often relies on the operator's tactile sensation. Consequently, in cases where the blood vessel's diameter is narrow, the vessel wall has low elasticity, or the vessel wall is calcified and hardened, the needle tip may fail to reach the vessel lumen. Complications of venipuncture include nerve damage, vasovagal reactions, infections, subcutaneous hematomas, and allergies, with fatalities being rare. However, in procedures that involve needle insertion into the body's central regions, such as central venous catheter (CVC) placement or pericardiocentesis, despite using imaging guidance like X-rays or ultrasound, the mortality rate can be high. Complications associated with CVC include infections, thrombosis, and mechanical complications. Atypical mechanical complications include arterial puncture, pneumothorax, hematoma, and hemothorax, with an incidence rate of up to 19% [1]. Pericardiocentesis complications encompass pneumothorax, damage to surrounding vital organs, cardiac wall puncture, and death. Before the advent of echocardiographic guidance, pericardiocentesis primarily relied on a blind approach, with a life-threatening complication rate exceeding 20% and a mortality rate of approximately 6% [2]. Currently, with the widespread use of echocardiographic guidance, the complication rate for pericardiocentesis has decreased to 5%, and the mortality rate has dropped to 1%. However, understanding ultrasound images requires specialized knowledge and experience, and it may be challenging to visualize in obese patients. Additionally, while 18-gauge needles were traditionally used for pericardiocentesis, the current trend is to use thinner 21G needles [3]. The 21G needle has probrems that are more prone to bending and breaking. The causes of complications during needle insertion can be attributed to various factors, including the operator's mental state, mechanical factors such as needle targeting errors (needle misplacement), infections, thrombosis, and others. Targeting errors, a mechanical factor, are a crucial factor that significantly impacts treatment efficacy and diagnostic accuracy. Targeting errors have been shown to arise from limitations in imaging, image misalignment, target uncertainty, human errors, target displacement due to tissue deformation, and needle deflection [4-7]. To mitigate targeting errors, extensive research has been conducted on automating needle insertion using robotic systems.

Needle insertion robots often employ MRI, CT, or ultrasound imaging to guide the needle toward the target [8-11]. However, image-guided needle targeting is difficult in obese patients and in cases with hardened tissue due to calcification, as halation may obscure the target or prevent tracking of the needle tip. During blind needle insertion, physicians typically hold the base of the needle and rely on the force feedback perceived by their fingers to estimate the needle's deflection and perform targeting. Therefore, we propose a method that generates needle trajectories and controls the needle based on force feedback, similar to how physicians manipulate needles during blind insertions. In this proposed method, MRI, CT, and ultrasound imaging are utilized as supplementary aids to improve insertion accuracy by tracking the target.

Therefore, given the high incidence of severe complications and the challenging nature of needle targeting due to respiratory motion in pericardiocentesis, our last goal was set to develop an robotic needle insertion system that used force feedback for needle control for pericardiocentesis. Our initial objective is to estimate the needle tip position using force feedback and propose a robust needle control method against external forces during insertion. Leveraging force feedback for needle tip position estimation and control can also serve as a training tool for needle insertion procedures. Additionally, it offers a wide range of applications, such as quantitatively evaluating the differences between experienced and inexperienced operators, integrating augmented reality (AR) to provide guidance during human-performed insertions, and supporting other potential applications. By utilizing force feedback, our

approach not only addresses the challenges of needle targeting but also presents opportunities for training, assessment, and assistive technologies in the field of needle-based interventions.

1.2 Proposal of Needle Control Method to Decrease Needle Deflection

The proposed method for reducing needle deflection is shown in Figure 1. This research is divided into two sections. The first section aims to estimate the vector of the needle deflection caused by external forces using artificial intelligence. Here we explain the needle deflection vector. When observing from the needle base to the needle tip, if the needle tip was bent away from the needle's long axis, as shown in Figure 2, the needle tip can be represented on a two-dimensional plane with the needle's axis as the origin [12]. In this study, we refer to the vector from the origin of this plane to the needle tip as the needle deflection vector. The needle deflection vector can be calculated using the following equation,

$$\vec{v}_B = \vec{v}_T - \vec{v}_R \cdots\cdots\cdots\cdots\cdots\cdots (1)$$

Where $\vec{v}_B$ is the needle deflection vector, $\vec{v}_T$ is the position vector of the needle tip measured using a 3D position tracking system, and $\vec{v}_R$ is the projection vector of $\vec{v}_T$ relative to the vector between the needle base starting position and the target position.

The input for the first artificial intelligence (AI 1) includes the forces acting around the needle base, the position of the needle base, and et al. The output consists of the estimation of the needle deflection vector at the current time. Regarding Section 1, in our previous report, we elucidated whether it is possible to estimate the needle deflection vector using artificial intelligence[13].

The second section aims to determine whether a needle base position can be derived using a artificial intelligence to reduce the needle deflection. In this research, we employed a Long Short-Term Memory (LSTM) model. LSTM is a type of recurrent neural network (RNN) architecture, designed to overcome the limitations of traditional RNNs in capturing long-term dependencies in sequential data. In an LSTM network, there are special units, known as memory cells, which are capable of maintaining information over long periods of time. The memory units of LSTM networks resemble the way humans store and recall memories when learning behaviors, which led us to hypothesize that they could be effective for our current objective. An LSTM is made up of 3 gates, Input Gate, Forget Gate, Output Gate. The equations for an LSTM block are shown as follows:

$$f_t = \sigma(W_f[h_{t-1}, x_t] + b_f) \cdots\cdots\cdots (2)$$

$$i_t = \sigma(W_i[h_{t-1}, x_t] + b_i) \cdots\cdots\cdots (3)$$

$$o_t = \sigma(W_o[h_{t-1}, x_t] + b_o) \cdots\cdots\cdots (4)$$

$$\tilde{C}_t = tanh(W_C[h_{t-1}, x_t] + b_C) \cdots (5)$$

$$C_t = f_t * C_{t-1} + i_t * \tilde{C}_t \cdots\cdots\cdots\cdots (6)$$

$$h_t = o_t * \tanh(C_t) \cdots\cdots\cdots\cdots\cdots (7)$$

where f_t is the forget gate, i_t is the input gate, o_t is the output gate, $\tilde{C}_t$ is the candidate for cell state at timestamp t, C_t is the cell state at t, σ is the sigmoid function, W_x is the weight for the respective gate(x) neurons, h_{t-1} is the output of the previous lstm block, x_t is the input at current t, b_C is the biases for the respective gates(x), h_t is the output of the current lstm block.

The input, x_t for the second artificial intelligence (AI 2) includes the forces and torques acting around the needle base, the insertion depths of the needle tip and the inversion of the needle deflection vector estimated by AI 1. The output, h_t consists of the estimated position of the needle base to reduce the needle deflection at the current timestamp.

In this report, before proposing a method to estimate the needle base position that reduces the needle deflection vector in the second section, we must first clarify whether it is possible to estimate the needle base position that generates the current needle deflection vector using machine learning, and then report on the accuracy of the method.

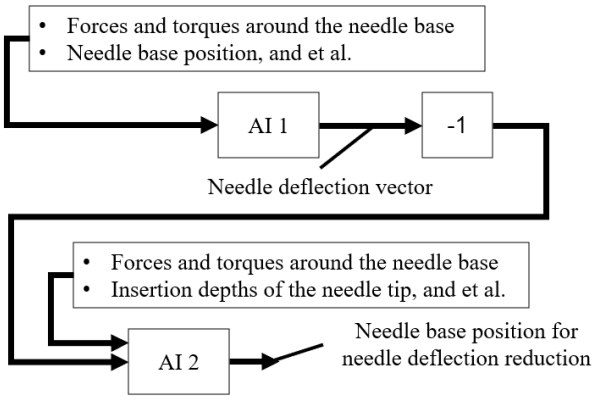

Fig.1 Schematic diagram of needle control method to reduce needle deflection.

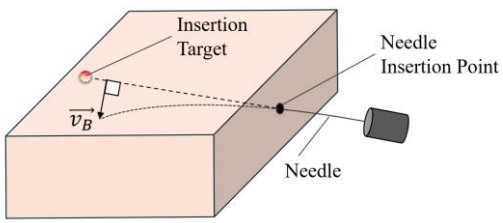

Fig.2 Needle deflection vector.

2. Experiment

2.1 Experimental Equipment and Conditions

The experimental equipment was shown in Figure 3. This experimental setup was used get the traning data for LSTM model. The 6-axis force sensor used to measure Fx,y,z and $\tau x,y,z$ was set near the base of the needle. The needle used was a 21G type needle usually used for percutaneous transhepatic cholangiography drainage. The needle tip and needle base positions were measured using a magnetic type 3D position tracking system (AURORA SYSTEM, NDI). 6-degree-of-freedom (DOF) type and 5DOF type position sensors were used. In a previous research, the needle insertion phantom was made using materials such as gelatin gel, PVA, silicone rubber, and so on [13]. We decided to use gelatin for the phantom in this experiment because it is inexpensive and it is easy to adjust its hardness. A gelatin phantom with a concentration of 15% was used for this experiment. During the needle insertion into the phantom, an external force was manually applied to the top face of the phantom. The dataset was obtained by inserting the needle into six points on the phantom surface perpendicular to the area where the external force was applied as shown in Figure 3. The black dots in Figure 3 represents the needle insertion points for training data set, whereas the red dot represents the needle insertion point for the test data ($y = 40\ mm$, $z = 15\ mm$). The validation data used during the training of the LSTM model was collected from the coordinates $y = 10\ mm$, $z = 5.0\ mm$.

The experimental procedure was as follows:

1) The needle was set in front of the insertion surface of the phantom.
2) The needle was inserted into the phantom along the needle axial direction until a certain insertion depth L_1.
3) The needle base was moved downwards for a distance of vector $\vec{h}$.
4) The needle was moved along the needle axial direction until a certain insertion depth L_2.
5) The current phantom is then replaced by a new one and the experiment is repeated again from step 1 for all the values of L_1 and $\vec{h}$.

The deflection vector of the needle tip $\vec{v}_B$ was calculated by measuring the needle tip position and the needle base position. In this experiment, L_1, L_2 and $\vec{h}$ were calculated using a motor encoder. Throughout the experiment, L_2 was kept at a constant value of 50 mm. L_1 and $\vec{h}$ were each divided into three discreet values. L_1 values included 10 mm, 30 mm, 50 mm, while $\vec{h}$ values included 5 mm, 10 mm, 15 mm. Given that there are 6 puncture sites on the gelatin and each puncture site has 9 conditions each, a total of fifty-four training data were collected. The root mean squared error (RMSE) was used for evaluating the accuracy of the estimated results.

As explained in section 1.2, the input to the LSTM model x_t includes the forces $Fx,y,z(t)$ and torques $\tau x,y,z(t)$ around the needle base, the insertion depth of the needle L_1 and the needle tip deflection vector $\vec{v}_B$. The output of this LSTM model was set as the needle base vector $h(t)$. The hyperparameters of the LSTM model were tuned automatically using Optuna (Preferred Networks), an open-source automatic hyperparameter optimization framework.

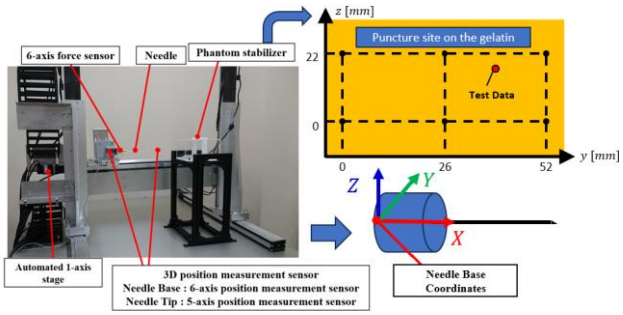

Fig.3 Experimental equipment

2.2 Results

The time-series data results estimating the position of the needle base are shown in Figures 4 and 5. Figure 4 shows the Y-axis component, and Figure 5 shows the Z-axis component. The orange line represents the estimated values, the blue line represents the actual measured values, and the green line represents the error values obtained by subtracting the measured values from the estimated values. From Figure 4, the mean error for the Y-axis component was 0.14 ± 0.20 mm. The error value in the Y-axis component increased when the needle base is stationary, as seen from the time range 20 s to 30s. From Figure 5, the mean error for the Z-axis component was -0.45 $\pm$ 1.20 mm. When the needle base was stationary, the error in the Z-axis component was close to zero, as seen from the time range 20 s to 30 s. The overall root mean squared error (RMSE) of the results was 0.92 mm.

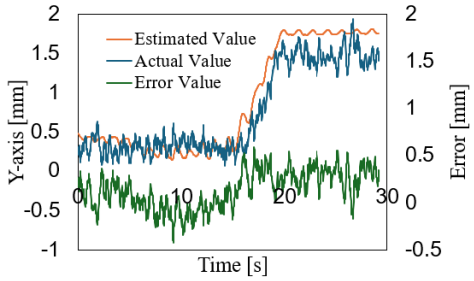

Fig.4 Prediction result (Y axis)

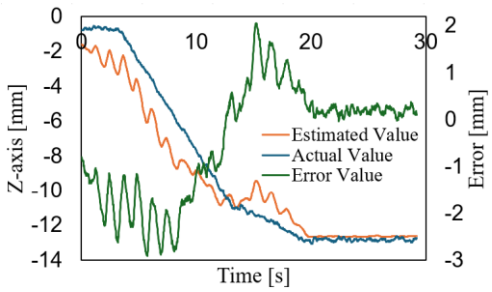

Fig.5 Prediction result (Z axis)

3. Discussion

When the needle base position was moved in the Z-axis direction, the error in the estimation results for the Z-axis component of the needle base position increased. One possible cause for this is that the movement of the needle base in the Z-axis direction caused the needle to bend, resulting in non-linear changes in torque at the base of the needle. In our method, the position of the needle base needs to be controlled based on the estimation results of the needle deflection. However, if the error is large, as observed in the present results, it becomes difficult to sufficiently reduce the needle deflection, and the needle tip may not reach the target. Therefore, improving the estimation accuracy when the needle base is moved in the Z-axis direction is an important element in this research. In recent years, ensemble learning has been extensively studied, but in the present research, we believe that the data used to train the AI needs to be divided into smaller tasks. For example, with and without external forces, the needle base is moved in each axis (X, Y, Z) direction, and different AIs can be trained for each condition, which can then be merged to create an integrated AI. Another reason for the low estimation accuracy is that feature selection was not fully implemented in this study. The features provided to the AI are an important factor that affects the estimation accuracy, so it will be necessary to examine the features in the future.

4. Conclusion

The ultimate goal of this research is to develop a robot that can automate pericardiocentesis, and in this report, we verified whether it is possible to estimate the position of the needle base that can reduce needle deflection based on force information. As a result of the experiments, a problem arose where the estimation accuracy decreased when the position of the needle base was moved. In the future, we plan to consider ensemble learning and other estimation methods to improve the estimation accuracy.

Acknowledgement

This work was supported by JSPS KAKENHI Grant Number JP21K18087.

Reference

1) Nguyen CT, Lee E, Luo H, Siegel RJ, “Echocardiographic guidance for diagnostic and therapeutic percutaneous procedures”, Cardiovasc Diagn Ther, Vol.1, No.1, pp.11-36, 2011.
2) Kumar R, Sinha A, Lin MJ, Uchino R, Butryn T, O'Mara MS, Nanda S, Shirani J, Stawicki SP, “Complications of pericardiocentesis: A clinical synopsis”, Int J Crit Illn Inj Sci, Vol.5, No.3, pp.206-212, 2015.
3) Morton Kern, Andrew Doorey, “Conversations in Cardiology: Should We Use Micropuncture Technique for Pericardiocentesis?”, Cath Lab Digest, Vol.23, No.9, 2015.
4) H. K. Hussain, J.E.Kingston, P. Domizio, A.J.Norton, R. H. Reznek, “Imaging-guided core biopsy for the diagnosis of malignant tumors in pediatric patients”, American journal of roentgenology, Vol.176, No.1, pp.43-47, 2001.
5) P. L. Roberson, V. Narayana, D. L. McShan, R. J. Winfield, P. W. McLaughlin, “Source placement error for permanent implant of the prostate”, Medical Physics, Vol.24, No.2, pp251-257, 1997.
6) R. Taschereau, J. Pouliot, D. Tremblay, “Seed misplacement and stabilizing needles in transperineal permanent prostate implants”, Radiotherapy and Oncology: Journal of the European Society for Therapeutic Radiology and Oncology, Vol.55, No.1, pp.59-63, 2000.
7) J. J. Carr, P. F. Hemler, P. W. Halford, R. I. Freimanis , R. H. Choplin, M. Y. Chen, “Stereotactic localization of breast lesions: how it works and methods to improve accuracy”, Radiographics: A Review Publication of the Radiological Society of North America, Inc, Vol.21, No.2, pp.463-473, 2001.
8) Samuel Lafreniere, Olivia Lee Sprouse, Ryan Justin Padilla, Bardia Konh, “DESIGN OF AN MRI-COMPATIBLE ROBOT FOR IMAGE-GUIDED NEEDLE INSERTION PROCEDURES USING ACTIVE TENDON-DRIVEN NEEDLES”, 2023 Design of Medical Devices Conference, 2023.
9) Pedro Moreira, Leanne Kuil, Pedro Dias, Ronald Borra, Sarthak Misra, “Tele-Operated MRI-Guided Needle Insertion for Prostate Interventions”, Journal of Medical Robotics Research, Vol.4, No.1, 2019.
10) Hajime Ishii, Tetsushi Kamegawa, Hiroki Kitamura, Takayuki Matsuno, Takao Hiraki, Akio Gofuku, “Development of a prototype of puncturing robot for CT-guided intervention”, 2016 IEEE 11th Conference on Industrial Electronics and Applications (ICIEA), pp1020-1025, 2016,
11) Meaghan Bowthorpe, Mahdi Tavakoli, Harald Becher, Robert Howe, “Smith predictor based control in teleoperated image-guided beating-heart surgery”, 2013 IEEE International Conference on Robotics and Automation (ICRA), pp. 5825-5830, 2013.
12) Hiroyuki Kataoka, Toshikatsu Washio, Michel Audette & Kazuyuki Mizuhara, “A Model for Relations Between Needle Deflection, Force, and Thickness on Needle Penetration”, Medical Image Computing and Computer-Assisted Intervention – MICCAI 2001, Vol.2208, pp.966-974, 2001.

13) Axel Yap Shen Yit, Yuta Fukushima. “Proposal of a needle deflection estimation method during needle insertion using AI - Examination of estimation accuracy based on differences in input information to AI -”, JSMBE Symposium 2023, C-09, 2023.